

Hydrogenation of CO on a silica surface: an embedded cluster approach

Article (Published Version)

Goumans, T P M, Catlow, C Richard A and Brown, Wendy A (2008) Hydrogenation of CO on a silica surface: an embedded cluster approach. *Journal of Chemical Physics*, 128 (13). ISSN 0021-9606

This version is available from Sussex Research Online: <http://sro.sussex.ac.uk/id/eprint/48676/>

This document is made available in accordance with publisher policies and may differ from the published version or from the version of record. If you wish to cite this item you are advised to consult the publisher's version. Please see the URL above for details on accessing the published version.

Copyright and reuse:

Sussex Research Online is a digital repository of the research output of the University.

Copyright and all moral rights to the version of the paper presented here belong to the individual author(s) and/or other copyright owners. To the extent reasonable and practicable, the material made available in SRO has been checked for eligibility before being made available.

Copies of full text items generally can be reproduced, displayed or performed and given to third parties in any format or medium for personal research or study, educational, or not-for-profit purposes without prior permission or charge, provided that the authors, title and full bibliographic details are credited, a hyperlink and/or URL is given for the original metadata page and the content is not changed in any way.

Hydrogenation of CO on a silica surface: An embedded cluster approach

T. P. M. Goumans, C. Richard A. Catlow, and Wendy A. Brown

Citation: *The Journal of Chemical Physics* **128**, 134709 (2008); doi: 10.1063/1.2888933

View online: <http://dx.doi.org/10.1063/1.2888933>

View Table of Contents: <http://scitation.aip.org/content/aip/journal/jcp/128/13?ver=pdfcov>

Published by the [AIP Publishing](#)

Articles you may be interested in

[Hydrogen activation, diffusion, and clustering on CeO₂\(111\): A DFT+U study](#)

J. Chem. Phys. **141**, 014703 (2014); 10.1063/1.4885546

[Effect of Zn on the adsorption of CO on Pd\(111\)](#)

J. Chem. Phys. **133**, 214702 (2010); 10.1063/1.3512631

[The importance of hydrogen's potential-energy surface and the strength of the forming R – H bond in surface hydrogenation reactions](#)

J. Chem. Phys. **124**, 044705 (2006); 10.1063/1.2159482

[Reactions and clustering of water with silica surface](#)

J. Chem. Phys. **122**, 144709 (2005); 10.1063/1.1878652

[General trends in CO dissociation on transition metal surfaces](#)

J. Chem. Phys. **114**, 8244 (2001); 10.1063/1.1372512



AIP | Journal of
Applied Physics

Journal of Applied Physics is pleased to
announce **André Anders** as its new Editor-in-Chief

Hydrogenation of CO on a silica surface: An embedded cluster approach

T. P. M. Goumans, C. Richard A. Catlow, and Wendy A. Brown^{a)}*Department of Chemistry, University College London, 20 Gordon Street, London WC1H 0AJ, United Kingdom*

(Received 21 November 2007; accepted 30 January 2008; published online 3 April 2008)

The sequential addition of H atoms to CO adsorbed on a siliceous edingtonite surface is studied with an embedded cluster approach, using density functional theory for the quantum mechanical (QM) cluster and a molecular force field for the molecular mechanical (MM) cluster. With this setup, calculated QM/MM adsorption energies are in agreement with previous calculations employing periodic boundary conditions. The catalytic effect of the siliceous edingtonite (100) surface on CO hydrogenation is assessed because of its relevance to astrochemistry. While adsorption of CO on a silanol group on the hydroxylated surface did not reduce the activation energy for the reaction with a H atom, a negatively charged defect on the surface is found to reduce the gas phase barriers for the hydrogenation of both CO and $\text{H}_2\text{C}=\text{O}$. The embedded cluster approach is shown to be a useful and flexible tool for studying reactions on (semi-)ionic surfaces and specific defects thereon. The methodology presented here could easily be applied to study reactions on silica surfaces that are of relevance to other scientific areas, such as biotoxicity of silica dust and geochemistry. © 2008 American Institute of Physics. [DOI: [10.1063/1.2888933](https://doi.org/10.1063/1.2888933)]

I. INTRODUCTION

Computational methods have facilitated detailed studies of reaction mechanisms in large systems such as nanostructures, enzymes, and heterogeneous catalysts.^{1–3} The division of a large system into a quantum mechanical (QM) and a molecular mechanical (MM) region (QM/MM) allows the reactive center to be studied with a high-level theory, while the effects of the environment (structural and electrostatic) are calculated at the computationally less-demanding MM level. QM/MM was first developed in the 1970s,⁴ and numerous variations of the method have been devised since (see Ref. 1 for a recent review with an extensive bibliography). In this paper, we use a QM/MM approach to assess the catalytic effect of a siliceous surface on an astrochemical reaction, the sequential hydrogenation of CO to form methanol.⁵ Although the calculations have been applied to astrochemical reactions, the present approach is applicable to detailed reactivity studies in a wide range of disciplines that involve siliceous surfaces. The biotoxicity of silica probably originates from the reactivity of surface sites, specifically silanol groups and undercoordinated silicon and oxygen atoms.⁶ Furthermore, silica's surface properties are of paramount importance in a variety of technological applications,⁷ and the dissolution and precipitation of the common mineral quartz have been widely investigated because of their major geochemical consequences.⁸

In the interstellar medium, molecular clouds are star-forming regions that display a rich variety of neutral molecules.⁹ The low temperatures (10–20 K or 20–100 K near a star-forming region) and pressures (10^{-15} mbar) found in these regions cause activated reactions to proceed very slowly. The chemistry of molecular clouds has been an active

research area over the last few decades, recently focusing on the role played by dust grains in catalysis.^{10,11} The dust grains, which are composed of either silicate or carbonaceous material,¹² apart from acting as a heat sink to stabilize exothermic reactions, also catalyze specific astrochemical reactions by reducing effective activation barriers. Methanol (CH_3OH) is one of the most abundant molecular species observed in the interstellar medium and is thought to be formed on the surface of dust grains.¹³ The suggested route of surface formation of CH_3OH is via the sequential addition of hydrogen atoms to adsorbed CO.¹⁴ However, experimental investigations of the formation of CH_3OH from the bombardment of CO ices with hydrogen atoms have shown different results,^{15,16} although both formaldehyde ($\text{H}_2\text{C}=\text{O}$) and CH_3OH have been observed as products at temperatures of 10–20 K. It has been suggested that the formation of hydrogenated products could also be affected by photons or charged particles from the atom source.¹⁶ Indeed, Hudson and Moore have shown that CH_3OH is formed efficiently upon irradiating a mixed CO:H₂O ice with 0.8 MeV protons.¹⁷ The influence of water ice on the formation of CH_3OH has been shown to be negligible in a previous computational study.¹⁸ Here, we use QM/MM to assess whether a siliceous surface can specifically catalyze the formation of CH_3OH . As a model siliceous surface, we use the hydrogenated (100) surface of edingtonite, a naturally occurring zeolite,¹⁹ which is a good computational model for an amorphous silica surface.²⁰ We also consider negatively charged and radical defect surface sites as potential catalytic sites. Previously, we have reported the catalytic effect of a negatively charged silica site on the hydrogenation of CO. In this paper, we give a complete account of the methodology used and explore the surface reactions on the hydrogenated and radicaloid surface sites, in addition to the negatively charged surface site, in detail.

^{a)}Electronic mail: w.a.brown@ucl.ac.uk.

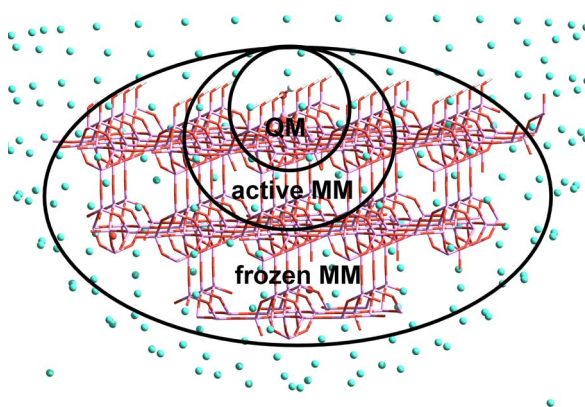


FIG. 1. (Color online) QM/MM cluster setup. The figure shows a 25 Å radius hemispherical surface cluster cut from the hydroxylated (100) surface of edingtonite, with correcting charges, divided into three regions.

II. METHODOLOGY

The QM/MM calculations are set up within CHEMSHELL,³ a modular approach that provides great flexibility for choosing the QM code, the Hamiltonian and basis set, the MM code and force field parameters, the QM/MM interface, and the optimization algorithms. The CHEMSHELL code is a valuable computational tool for surface chemistry, with applications ranging from astrochemistry to industrial catalysis.^{2,3,5,21} In this paper, we study the reactivity of active charged and radical silica surface sites, which are also indicated in the biotoxicity of silica.^{6,7,22} The described computational approach could augment recent QM-cluster calculations that study the reactivity of those surface sites^{6,22} because the embedding scheme takes account of the structural and electrostatic effect of the surrounding solid. The QM/MM approach has the advantage of modeling the reactive site with accurate QM methods, while maintaining the embedding in the steric and electronic environment of the solid state with low-cost MM methods. Most importantly, in an embedded cluster approach, charged surface defects are perfectly isolated, whereas periodic boundary programs have to cope with the periodic images of the defects potentially influencing one another, especially for charged defects.

A. Setup

The (100) surface of edingtonite is fully hydroxylated and optimized at the MM level. A hemispherical cluster with a radius of 25 Å is cut from this surface and is surrounded by small point charges to restore the Madelung potential (Fig. 1). We employ GAMESS-UK with the B97-1 functional²³ for our QM cluster because it has been shown to give good activation energies for hydrogen addition reactions.²⁴ A 6-31+G** (5D) basis was used for the adsorbates and the O and H atoms of the reactive surface sites, and a 6-31G* (5D) basis is employed for the remainder of the QM cluster. The QM cluster is electrostatically embedded in a MM cluster which is treated with the DL_POLY code with a modified Hill-Sauer force field.²⁵ The link-atom and charge-shifting scheme, as developed for zeolites, is employed at the QM/MM boundary.³ The energies and gradients of the embedded cluster are evaluated as a sum of the QM and MM

TABLE I. Force field parameters used in this study.

Charges		
Si: 1.2, O: -0.6, H: 0.3		
Harmonic stretch		
O-Si:	$k=28.9868 \text{ eV/\AA}$,	$r_{\text{eq}}=1.6104 \text{ \AA}$
H-O:	$k=110.4 \text{ eV/\AA}$,	$r_{\text{eq}}=0.95 \text{ \AA}$
Harmonic angle-bending		
O-Si-O:	$k=7.8976 \text{ eV/rad}^2$,	$\theta_{\text{eq}}=112.0^\circ$
Si-O-Si:	$k=7.8542 \text{ eV/rad}^2$,	$\theta_{\text{eq}}=140.0^\circ$
Si-O-H:	$k=2.6036 \text{ eV/rad}^2$,	$\theta_{\text{eq}}=118.9^\circ$
Lennard-Jones 9-6 potentials		
Si-Si:	$C^9=8110.7120 \text{ eV} \times \text{\AA}^9$	
H-O:	$C^9=136.99573 \text{ eV} \times \text{\AA}^9$	
H-Si:	$C^9=393.36426 \text{ eV} \times \text{\AA}^9$	
O-Si:	$C^9=4495.1556 \text{ eV} \times \text{\AA}^9$	
O-O:	$C^9=2491.3239 \text{ eV} \times \text{\AA}^9$, $C^6=169.23447 \text{ eV} \times \text{\AA}^6$	

energies (additive scheme). Transition states are optimized with the Baker algorithm (see below),²⁶ and all stationary points are characterized by calculating the frequencies of the entire active site (QM+MM) numerically. Unscaled zero-point energy corrections are included and reaction and activation energies are reported in kJ/mol. Different QM-cluster and active MM-region sizes have been considered to ensure that no artifacts arise from the QM/MM partitioning.

B. MM parameters

In CHEMSHELL, spherical bulk clusters and hemispherical surface clusters of covalent solids are conveniently generated with an automatic assignment of the connectivity within DL_POLY, assuring a consistent assignment of charges. Therefore, we chose to use the Hill-Sauer potentials,²⁵ which have been used for QM/MM studies of zeolites.^{2,3,27} However, it was necessary to truncate the complex potentials for use with MARVIN (Ref. 28) and GULP (Ref. 29) to generate and study the surfaces within CHEMSHELL. All cubic and quartic force constants, torsional parameters, and cross terms were eliminated. This truncated force field necessitated the inclusion of an attractive O-O Lennard-Jones term to reproduce the lattice parameters of α -quartz. These parameters were optimized by fitting to α -quartz structural data (lattice parameters, bond lengths, and angles)³⁰ using the GULP code.²⁹ Likewise, the parameters involving the H atoms were also optimized to reproduce the structure of the hydroxylated (001) α -quartz surface at the density functional theory (DFT) level.³¹ The resulting parameters are reported in Table I.

C. Validation

To validate the use of these MM parameters in a QM/MM setup, the hydrogarnet defect was studied initially. This defect is formed by the reaction $\text{SiO}_2 + 2\text{H}_2\text{O}(\text{l}) \rightarrow \text{hydrogarnet} + 1/3 \alpha\text{-SiO}_2$, where four OH groups form a cluster in a Si vacancy. The hydrogarnet defect was considered in the center of a sphere with a radius of 29 Å and the QM cluster included all O-Si units linking to the Si-atom or hydrogarnet defect. The B3LYP functional with a large basis

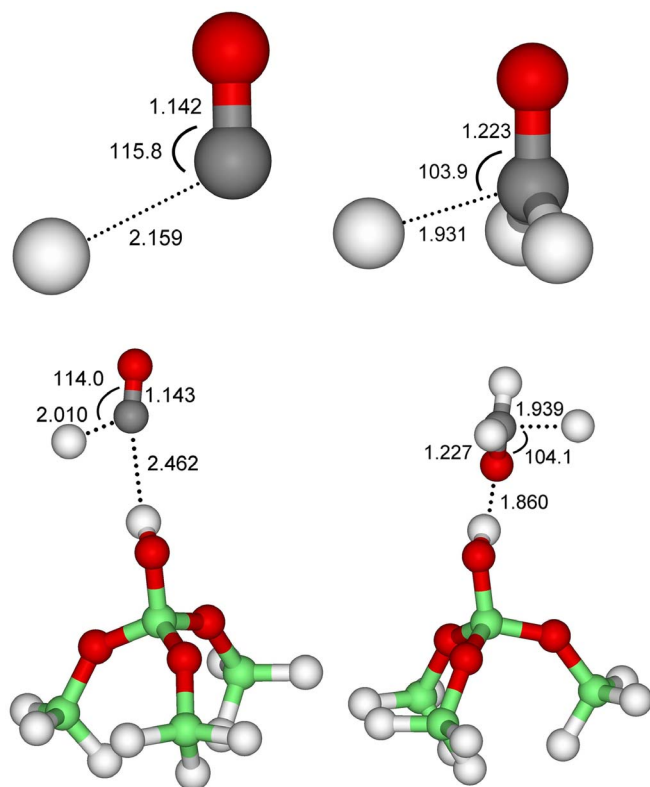


FIG. 2. (Color online) Transition state geometries of the QM region for H + CO (left) and H + H₂CO (right) in the gas phase (top) and adsorbed on a SiOH surface defect (bottom). Bond lengths are indicated in Å, angles in degrees. White, H; light gray (green), Si; dark gray (red), O; and gray, C.

set on the central Si (88-1111G*), O (8-411G*), and H atoms (8-21G**) (Ref. 32) was used, with a 6-31G* basis set on all other atoms. The structure and energy of bulk α -quartz was calculated with CRYSTAL.³³ The energy of the hydrogarnet defect thus calculated was 52–55 kJ/mol, depending on the size of the active MM region. This value is in agreement with periodic DFT calculations for the energy of the hydrogarnet defect in α -quartz by de Leeuw (63 kJ/mol, PW91)³⁴ and the hydrogarnet defect in sodalite by Pascale *et al.* (48 kJ/mol, B3LYP).³⁵

To assess the validity of the QM/MM setup for surfaces, the adsorption energy of NH₃ on a silanol surface site was calculated and compared with the periodic DFT values of Ugliengo and co-workers on the same surface.²⁰ An 18 atom QM cluster of the surface site HOSi(OSiH₃)₃ was surrounded by an active MM cluster of 15 atoms (the O–Si units directly extending from the QM cluster). The active QM/MM site was embedded in an inactive MM cluster of 817 atoms and 233 point charges. With this approach, the calculated adsorption energy of NH₃ is 45.3 kJ/mol without zero-point energy correction, which is, considering the different basis set and functional, in good agreement with the previously calculated value of 49.3 kJ/mol.²⁰ The experimental adsorption energy of NH₃ on silica is 37 kJ/mol.³⁶

The influence of the size of the QM and MM clusters was tested using the adsorption energy of CO and the activation energy of the H + CO_{ads} reaction. With the above setup (18 QM + 15 MM atoms), the adsorption energy of CO is 6.5 kJ/mol without zero-point energy correction (3.8 kJ/mol

with zero-point energy corrections added). When the QM cluster is extended by making all active atoms QM atoms, the adsorption energy increases to 9.3 kJ/mol without zero-point energy corrections. Extending this larger QM cluster by including the next “layer” of SiO units as active MM atoms (27 atoms in total) hardly affects the CO adsorption energy (8.9 kJ/mol). Although the larger QM cluster gives an adsorption energy in closer agreement with experimental energies of CO on hydroxylated silicate material from comets (13.5 ± 3.0 kJ/mol),³⁷ the activation energy for the H + CO_{ads} reaction is exactly the same (14.6 kJ/mol without zero-point energy correction) for both the small QM cluster (18 QM + 15 MM) and the larger QM cluster (39 QM atoms). Since the aim of this study is to assess the catalytic effect of the surface, i.e. the change in the activation barrier for the surface reaction with respect to the gas phase reaction, the computationally less-demanding 18 QM + 15 MM cluster was used.

D. Transition state optimization algorithms

To determine the transition states (TSs), the most efficient approach was as follows:

- (1) Perform a constrained scan along the reaction coordinate, where the SiO(H) and adsorbate atoms are fully relaxed, while decreasing the distance between the incoming hydrogen atom and the carbon atom from ~ 2.5 to 1.75 Å. In this study, we only consider the Eley–Rideal mechanism, whereby the hydrogen atom originates from the gas phase.
- (2) Determine the maximum on this potential energy curve, calculate the Hessian for the same reduced set of active atoms, and optimize to a TS with the Baker algorithm.²⁶
- (3) Calculate the Hessian and optimize the TS for the full active site.
- (4) Calculate a full Hessian of the stationary points to ascertain the nature of the TS and to obtain zero-point energies.

For certain TSs, the microiterative scheme implemented in the hybrid delocalized internal coordinate optimizer³⁸ (HDLC-opt) may be quicker than performing steps (2) and (3). In this scheme, the Hessian is only calculated and updated for a chosen active core (partitioned rational function optimization), while the remainder of the active site is relaxed in between (Broyden–Fletcher–Goldfarb–Shanno) TS search steps. We found that the HDLC-opt scheme was effective in getting close to the TS quickly in most cases where the initial structure was not too far from the saddle point, but for the final optimization, the Baker algorithm was needed to minimize the gradients efficiently.

The largest computational effort in determining the reaction mechanisms is the calculation of the initial Hessian matrix for the TS optimization algorithms and the frequencies at the stationary points. Developments are currently underway to parallelize the numerical second derivatives as well as TS searching algorithms for efficient calculations on high-performance computing systems. Because the TS calcula-

TABLE II. Calculated activation (ΔE^\ddagger) and reaction energies (ΔE_{react}) in kJ/mol for the consecutive hydrogenation of CO in the gas phase and on different surface sites via the Eley–Rideal mechanism. For each reaction, the energies are given with respect to the adsorbed reactant.

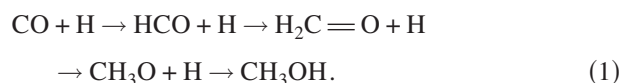
State	H+CO→HCO		H+HCO→H ₂ CO		H+H ₂ CO→H ₃ CO		H+CH ₃ O→H ₃ COH	
	ΔE^\ddagger	ΔE_{react}	ΔE^\ddagger	ΔE_{react}	ΔE^\ddagger	ΔE_{react}	ΔE^\ddagger	ΔE_{react}
Gas phase	15.6	−79.1	0	−356.5	21.9	−100.5	0	−407.4
ads SiOH	16.3	−77.2	0	−367.5	22.8	−101.5	0	−410.6
ads SiO [−]	9.5	−132.1	0	−477.2	18.5	−130.5	0	−381.8
ads SiO*	0	−381.7	40.7	−39.0	0	−403.7	144.3	0.9

tions are very computationally demanding, we focus mainly on the reaction coordinates where the incoming hydrogen atom reacts with the adsorbate, while considering different lines of approach.

III. RESULTS AND DISCUSSION

A. Gas phase

The proposed formation pathway for CH₃OH in the interstellar medium, both in the gas phase and on the surface of a dust grain, is via the sequential addition of hydrogen atoms,^{14,18}



In this sequence, the first (H+CO) and third (H+H₂C=O) steps are activated in the gas phase, and these barriers are not reduced on a model water ice surface.¹⁸ We have previously shown that with our DFT approach, B97-1/6-31+G**, the calculated gas phase activation barriers for these reactions are in good agreement with high-level *ab initio* results.⁵ The structures of the gas phase TSs are shown in Fig. 2. The H+CO TS is very early on the potential energy surface (PES), as indicated by the long H⋯CO distance and the exceptionally small stretching (0.003 Å) of the reactant CO bond. For H+H₂CO, the TS is a little later, with a significantly shorter H⋯CO distance and a 0.013 Å elongation of the reactant CO double bond. In both cases, the hydrogen atom approaches an angle close to that of the product geometry. The gas phase reaction and activation barriers for each of the steps in Eq. (1) are reported in Table II, along with the respective values for the surface reactions (discussed below). With the two gas phase barriers of 15.6 and 21.9 kJ/mol for the first and third hydrogen addition reactions, respectively, the classical rate of CH₃OH formation is negligible at the low temperatures of 10–20 K prevalent in molecular clouds. However, tunneling through the reaction barriers is likely to

play an important role at these low temperatures.^{18,39,40}

B. Surface reactions

The effect of a siliceous surface on the formation of CH₃OH via Eq. (1) was assessed with QM/MM calculations on a hydroxylated edingtonite surface, with the setup as described in Sec. II. We also considered the effect of the surface defects SiO[•] and SiO[−], when the species that react with the incoming hydrogen atom are adsorbed on this defect site. The results for the negatively charged SiO[−] defect have been reported previously.⁵ The adsorption energies of all reaction intermediates on the SiOH, SiO[•], and SiO[−] sites are reported in Table III. All activation and reaction energies for each of the reaction steps in the gas phase and on the three surface sites are summarized in Table II, while the structures of the TSs are given in Figs. 2 and 3.

1. SiOH surface site

The reaction and activation energies for the formation of CH₃OH via Eq. (1) on a silanol surface site are virtually identical to the respective gas phase energies (Table II). Likewise, the geometric features of the TS of the surface reactants are close to those of the gas phase TSs (Fig. 2). Only the H⋯CO_{ads} distance for the H+CO_{ads} TS is significantly shortened with respect to the gas phase reaction, but the activation energy remains the same. All reaction intermediates are weakly physisorbed on the SiOH group ($E_{\text{ads}} = 2\text{--}17$ kJ/mol, Table III); therefore, the PESs for the hydrogen addition reactions are not strongly perturbed by adsorption on a silanol surface site. For this surface site, the most important catalytic effect of the surface is to reduce the “effective reaction volume” for the hydrogen atom by increasing the collision frequency on the surface with respect to the gas phase, where collisions are scarce at pressures of $\sim 10^{-15}$ mbar.⁴¹

TABLE III. Calculated adsorption energies in kJ/mol for the reaction intermediates for the hydrogenation of CO on different surface sites.

Site	CO	HCO	H ₂ C=O	CH ₃ O	CH ₃ OH
SiOH	3.8	1.9	12.9	13.9	17.0
SiO [−]	18.1	71.2	50.2	72.8 ^a	54.6
SiO*	133.2	435.8	118.3	418.4	13.1

^aThis species barrierlessly rearranges to SiOH⋯H₂CO[•], which is 3.5 kJ/mol lower in energy (Ref. 5).

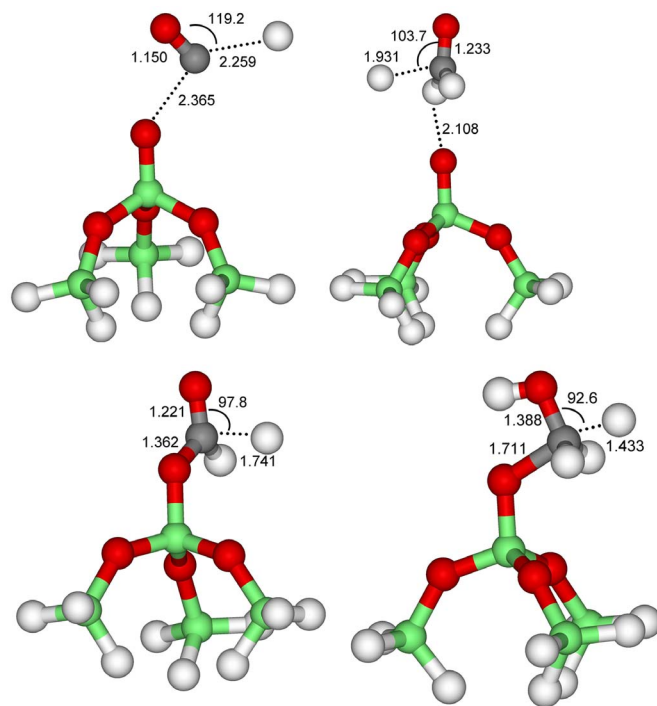


FIG. 3. (Color online) Transition state geometries of the QM region for $\text{H} + \text{CO}_{\text{ads}}$ (left) and $\text{H} + \text{H}_2\text{CO}_{\text{ads}}$ (right) on the SiO^- (bottom) and SiO^\cdot (top) surface defects. Bond lengths are indicated in Å, angles in degrees. White, H; light gray (green), Si; dark gray (red), O; and gray: C.

2. SiO^- surface site

When a proton is removed from the SiOH group, the negatively charged silanolate surface defect effectively lowers the activation energy for $\text{H} + \text{CO}_{\text{ads}}$ and $\text{H} + \text{H}_2\text{C}=\text{O}_{\text{ads}}$ by 6.8 and 4.3 kJ/mol, respectively (Table II). In Fig. 3, the structures of the two transition states are shown. Comparing the distances of the developing $\text{H} \cdots \text{C}$ bonds of the TS geometries for the surface reactions with the gas phase structures (Fig. 2), it appears that the $\text{H} + \text{CO}_{\text{ads}}$ TS is slightly earlier. More significantly, the CO bond is stretched in both surface TSs, indicating a weakening of the CO triple and $\text{H}_2\text{C}=\text{O}$ double bond by the negative charge. This weakening of the unsaturated bond, also shown by the redshift in the infrared frequencies,⁵ catalyzes the hydrogen addition reactions. Since dust grains are thought to bear negative charges,⁴² this catalytic effect, whereby a silanolate group activates unsaturated bonds, may be a ubiquitous mechanism for astrochemical hydrogenation reactions on the surface of dust grains. Furthermore, since the PESs are perturbed by the negatively charged defect, the tunneling probabilities through the barriers could also change.

3. SiO^\cdot surface site

Radicaloid sites are highly reactive, and since radical pairs are preferentially formed over ionic pairs upon silica fracture,²² the radical surface sites are indicated as the main contributors to the biotoxicity of silica dust.⁷ Recently, the reactivity of the radical SiO^\cdot and Si^\cdot sites, as well as the charged Si^+ and SiO^- sites, toward H_2O was studied computationally.²² Since the model QM cluster used in the previous calculations included intramolecular hydrogen

bonds, we cannot compare to their results directly. However, the SiO^\cdot defect was shown to be very reactive in the heterolytic splitting of H_2O . For the reaction considered here, the radicaloid SiO^\cdot surface site drastically changes the reaction mechanism for Eq. (1). The SiO^\cdot surface site reacts barrierlessly with an incoming hydrogen atom. Consequently, in the interstellar medium, most SiO^\cdot sites will be rehydrogenated to yield a silanol (SiOH) surface site. However, if a mobile CO is nearby, it can also chemisorb (133.2 kJ/mol) to the SiO^\cdot surface site without a barrier. In that case, a radicaloid intermediate $\text{SiO}-\text{C}^\cdot=\text{O}$ is formed, which has another carbon-oxygen bond and an unpaired electron centered on the carbon atom. This intermediate is still highly reactive and reacts without a barrier with an incoming hydrogen atom from either side. If the hydrogen atom is constrained to approach the SiO group from the opposite side to where CO is bonded, a silanol group (SiOH) may be formed and the CO is displaced. Alternatively, if the hydrogen atom approaches from the carbon side, the $\text{SiO}-\text{C}(\text{H})=\text{O}$ intermediate is formed in a barrierless radical-radical addition. For this intermediate, however, the reaction with the second H atom is now activated by 40.7 kJ/mol, yielding $\text{SiO}-\text{CH}_2-\text{O}^\cdot$. The structure of the TS (Fig. 3) reveals that this is a late TS compared to the other surface reactions, with a $\text{H} \cdots \text{C}$ distance of 1.741 Å. The third H addition to the radicaloid oxygen center ($\text{H} + \text{SiO}-\text{CH}_2-\text{O}^\cdot \rightarrow \text{SiO}-\text{CH}_2-\text{OH}$) is unactivated, while the fourth and final H addition is again strongly activated by 144.3 kJ/mol and is even slightly endothermic (Table II). This second TS is even later on the PES with a fairly developed $\text{H}-\text{C}$ bond (1.433 Å) and a considerably lengthened $\text{Si}-\text{C}$ chemical bond (Fig. 3). While a radical defect can entirely remove the activation barriers for the first and third hydrogen additions to CO, the introduction of the two new barriers for the second and fourth H additions makes this pathway prohibitive in the cold interstellar medium.

IV. CONCLUSIONS

Because of its relevance to astrochemistry, the hydrogenation of CO to form CH_3OH on surfaces has previously been studied both experimentally^{15,16} and computationally.¹⁸ In the gas phase, the formation of CH_3OH involves two activation barriers which are too high (15.6 and 21.9 kJ/mol) for this reaction to proceed effectively via a classical mechanism at the low temperatures in the interstellar medium.

Our embedded cluster approach has allowed us to assess the catalytic effect of a siliceous surface on this reaction. We have found that the silanol surface group (SiOH) has hardly any effect on the gas phase transition states and activation barriers. In contrast, a radicaloid SiO^\cdot surface site completely changes the reaction mechanism for the consecutive hydrogen addition reactions. The SiO^\cdot surface site is very reactive toward CO and once it is chemisorbed, CO can react barrierlessly with a H atom to yield chemisorbed HCO . Further hydrogenation of this intermediate, however, involves two more barriers (40.3 and 144.3 kJ/mol), rendering this to be an unlikely pathway to CH_3OH even at higher temperatures. However, the negatively charged SiO^- surface site was found

to be a good catalyst for CO hydrogenation. The adsorption energy of all reactants and reaction intermediates are increased by the SiO^- surface site. This enhanced interaction activates the CO triple and double bonds to effect a reduction of the $\text{H}+\text{CO}_{\text{ads}}$ and $\text{H}+\text{H}_2\text{C}=\text{O}_{\text{ads}}$ activation energies by 6.1 and 3.4 kJ/mol, respectively, which will accelerate the reaction.⁵ However, for a high efficacy at 10–20 K, the reactions are still required to tunnel efficiently through the activation barriers.

Because interstellar dust grains are likely to be negatively charged,⁴² and oxygen-rich dust grains are composed of silicates,¹² negatively charged SiO^- surface sites could be widespread catalytic sites in dusty molecular clouds. This site probably activates other multiple bonds as well and thereby promotes hydrogenation and oxidation of unsaturated species. We are currently investigating such processes for other relevant astrochemical reactions.

ACKNOWLEDGMENTS

The EPSRC is acknowledged for a post-doctoral fellowship for T.P.M.G. and for computer resources on HPCx used through the Materials Chemistry and UKCP consortia. We also thank the Davy Faraday Research Laboratory for the use of their computer resources. Paul Sherwood, Alexey Sokol, and Ben Slater, are acknowledged for their help with CHEM-SHELL. This work forms part of the research currently being undertaken in the UCL Centre for Cosmic Chemistry and Physics.

¹H. Lin and D. G. Truhlar, *Theor. Chem. Acc.* **117**, 185 (2007).

²J. To, P. Sherwood, A. A. Sokol, I. J. Bush, C. R. A. Catlow, H. J. J. van Dam, S. A. French, and M. F. Guest, *J. Mater. Chem.* **16**, 1919 (2006).

³P. Sherwood, A. H. de Vries, M. F. Guest, G. Schreckenbach, C. R. A. Catlow, S. A. French, A. A. Sokol, S. T. Bromley, W. Thiel, A. J. Turner, S. Billeter, F. Terstegen, S. Thiel, J. Kendrick, S. C. Rogers, J. Casci, M. Watson, F. King, E. Karlsen, M. Sjøvoll, A. Fahmi, A. Schafer, and C. Lennartz, *J. Mol. Struct.* **632**, 1 (2003).

⁴A. Warshel and M. Levitt, *J. Mol. Biol.* **103**, 227 (1976).

⁵T. P. M. Goumans, A. Wander, C. R. A. Catlow, and W. A. Brown, *Mon. Not. R. Astron. Soc.* **382**, 1829 (2007).

⁶V. Murashov, M. Harper, and E. Demchuk, *J. Occup. Environ. Hyg.* **3**, 718 (2006).

⁷A. P. Legrand, *The Surface Properties of Silica* (Wiley, New York, 1998).

⁸S. V. Yanina, K. M. Rosso, and P. Meakin, *Geochim. Cosmochim. Acta* **70**, 1113 (2006).

⁹E. Herbst, *J. Phys. Chem. A* **109**, 4017 (2005).

¹⁰D. A. Williams and E. Herbst, *Surf. Sci.* **500**, 823 (2002).

¹¹D. A. Williams, W. A. Brown, S. D. Price, J. M. C. Rawlings, and S. Viti,

Astron. Geophys. **48**(1), 25 (2007).

¹²B. T. Draine, *Annu. Rev. Astron. Astrophys.* **41**, 241 (2003).

¹³R. Garrod, I. H. Park, P. Caselli, and E. Herbst, *Faraday Discuss.* **133**, 51 (2006).

¹⁴A. G. G. M. Tielens and D. C. B. Whittet, *Molecules in Astrophysics*, edited by E. F. van Dishoeck (Kluwer, Dordrecht, 1997), p. 45.

¹⁵N. Watanabe, A. Nagaoka, T. Shiraki, and A. Kouchi, *Astrophys. J.* **616**, 638 (2004).

¹⁶K. Hiraoka, A. Wada, H. Kitagawa, M. Kamo, H. Unagiike, T. Ueno, T. Sugimoto, T. Enoura, N. Sogoshi, and S. Okazaki, *Astrophys. J.* **620**, 542 (2005).

¹⁷R. L. Hudson and M. H. Moore, *Icarus* **140**, 451 (1999).

¹⁸D. E. Woon, *Astrophys. J.* **569**, 541 (2002).

¹⁹W. M. Meier and D. H. Olson, *Atlas of Zeolite Structure Types* (Butterworth, London, 1987).

²⁰B. Civalleri and P. Uglierio, *J. Phys. Chem. B* **104**, 9491 (2000); P. Uglierio, B. Civalleri, R. Dovesi, and C. M. Zicovich-Wilson, *Phys. Chem. Chem. Phys.* **1**, 545 (1999).

²¹C. R. A. Catlow, S. A. French, A. A. Sokol, and J. M. Thomas, *Philos. Trans. R. Soc. London, Ser. A* **363**, 913 (2005).

²²J. Narayanasamy and J. D. Kubicki, *J. Phys. Chem. B* **109**, 21796 (2005).

²³F. A. Hamprecht, A. J. Cohen, D. J. Tozer, and N. C. Handy, *J. Chem. Phys.* **109**, 6264 (1998).

²⁴S. Andersson and M. Gruning, *J. Phys. Chem. A* **108**, 7621 (2004).

²⁵J. R. Hill and J. Sauer, *J. Phys. Chem.* **98**, 1238 (1994).

²⁶J. Baker, *J. Comput. Chem.* **7**, 385 (1986).

²⁷S. A. French, A. A. Sokol, S. T. Bromley, C. R. A. Catlow, and P. Sherwood, *Top. Catal.* **24**, 161 (2003).

²⁸D. H. Gay and A. L. Rohl, *J. Chem. Soc., Faraday Trans.* **91**, 925 (1995).

²⁹J. D. Gale, *Z. Kristallogr.* **220**, 552 (2005).

³⁰L. Levien, C. T. Prewitt, and D. J. Weidner, *Am. Mineral.* **65**, 920 (1980).

³¹T. P. M. Goumans, A. Wander, W. A. Brown, and C. R. A. Catlow, *Phys. Chem. Chem. Phys.* **9**, 2146 (2007).

³²See: <http://www.tcm.phy.cam.ac.uk/~mdt26/crystal.html>.

³³R. D. V. R. Saunders, C. Roetti, R. Orlando, C. M. Zicovich-Wilson, N. M. Harrison, K. Doll, B. Civalleri, I. J. Bush, Ph. D'Arco, and M. Llunell, CRYSTAL03, University of Torino, Torino 2003.

³⁴N. H. de Leeuw, *J. Phys. Chem. B* **105**, 9747 (2001).

³⁵F. Pascale, P. Uglierio, B. Civalleri, R. Orlando, P. D'Arco, and R. Dovesi, *J. Chem. Phys.* **117**, 5337 (2002).

³⁶W. Hertl and M. L. Hair, *J. Phys. Chem.* **72**, 4676 (1968).

³⁷M. N. Mautner, V. Abdelsayed, M. S. El-Shall, J. D. Thrower, S. D. Green, M. P. Collings, and M. R. S. McCoustra, *Faraday Discuss.* **133**, 103 (2006).

³⁸S. R. Billeter, A. J. Turner, and W. Thiel, *Phys. Chem. Chem. Phys.* **2**, 2177 (2000).

³⁹H. Hidaka, A. Kouchi, and N. Watanabe, *J. Chem. Phys.* **126**, 204707 (2007).

⁴⁰A. Tielens and W. Hagen, *Astron. Astrophys.* **114**, 245 (1982); T. I. Hasegawa, E. Herbst, and C. M. Leung, *Astrophys. J., Suppl.* **82**, 167 (1992).

⁴¹E. L. O. Bakes, *The Astrochemical Evolution of the Interstellar Medium* (Twin, Vledder, The Netherlands, 1997).

⁴²H. P. Gail and E. Sedlmayr, *Astron. Astrophys.* **41**, 359 (1975).